CHALMERS
UNIVERSITY OF TECHNOLOGY

Practical Aspects of Online Grid Impedance Estimation for HVDC Applications

Master thesis in Master Electric Power Engineering

Asim Ibrahim

Department of Electrical Engineering
CHALMERS UNIVERSITY OF TECHNOLOGY
Gothenburg, Sweden 2018

Master's thesis 2018:09

Practical Aspects of Online Grid Impedance Estimation for HVDC Applications

Asim Ibrahim

Department of Electric Engineering
Division of Electric Power Engineering
Chalmers University of Technology
Gothenburg, Sweden 2018

Practical Aspects of Online grid impedance estimation for HVDC applications
Asim Ibrahim

Supervisor: Pinaki Mitra, ABB HVDC
Examiner: Massimo Bongiorno, Electrical Engineering department

Master Thesis 2018:09
Department of Electric Engineering
Division of Electric Power Engineering
Chalmers University of Technology
SE-412 96 Gothenburg
Telephone +46 31 772 1000

Cover: Wind visualization constructed in Matlab showing a surface of constant wind speed along with streamlines of the flow.

Typeset in LaTeX
Printed by [Name of printing company]
Gothenburg, Sweden 2018

Practical aspects of online grid impedance estimation for HVDC applications
Asim Ibrahim
Department of Electrical Engineering
Chalmers University of Technology

Abstract

The purpose of this thesis work is to study different methods to perform online estimation of the grid impedance and to implement a suitable method for HVDC applications to verify the concept. An evaluation of these different methods is also presented with their advantages and disadvantages.
For HVDC applications, a steady-state method based on inter-harmonic current injection is selected to assess the grid impedance. This method has been selected because of its advantages over the other methods and also because of its suitability to the operational behavior of power systems.
A brief introduction of HVDC transmission system and its diverse technologies and topologies is presented to bring in the reader to the the topic. This introductory explanation provides an essential understanding of the basic concepts of HVDC transmission system operation. Special focus was given to the control system and modulation technique because of their importance in implementing this grid impedance evaluation technique.
An HVDC model developed by CIGRE working group B4-57 is used to implement the selected estimation technique. This estimation technique rely on inter-harmonic current injection. It consist of different stages.First, an inter-harmonic signal is to be generated. Then this signal is injected into the grid. The next step is to extract the specific injected inter-harmonic current and its corresponding voltage response. A system of known impedance and short circuit ratio (SCR) was used to evaluate the obtained results. Second order filters were tuned to extract the specific inter-harmonic voltage and current signals. Thereafter, the aforementioned extracted signals were fed to the impedance calculation algorithm, which is based on Ohm's law implemented using basic trigonometric identities to calculate the real and imaginary parts of the estimated impedance. Results from different system operational conditions were discussed and compared.
Implementing the estimation during system operation has been successfully addressed in this thesis work. Specific attention was given to the situation when the grid converts from moderately strong gird to a weak grid, where adaptation of the control parameters or a change in the control mode were required to maintain the stable performance of the system in different operational conditions.

Keywords: HVDC, Impedance, Inter-harmonic, .

Acknowledgements

First of all, I'd like to thank ABB for supporting this thesis work, and especially, Mr.Pankaj Roy, for his trust and support from the beginning of the thesis work.

My deepest gratitude goes to my supervisor Dr. Pinaki Mitra and my examiner professor Massimo Bongiorno for their guidance, advice and support throughout the whole thesis work.

The biggest gratitude and thankfulness go to My parents, everything in me is because of them. Their love, encourage and support are incomparable.

I would like to thank my friends and seniors at ABB Ahmed, Adil and Abdullahi for making my living in Ludvika enjoyable. Also, for sharing their passions and ideas.

Also, I'd like to thank the Swedish Institute for supporting my master studies with a generous scholarship and guidance for life and studies in Sweden.

Another warm thanking goes to my office-mate Anar Ibrayeva, for all the time we spent together full with PSCAD simulations. And also to my caring friend Amal.

Finally, I would like to thank everyone who had advised or guided me through my whole academic life, all the teachers, friends and everyone.

Asim Ibrahim, Ludvika, August 2018

Contents

List of Figures **xi**

List of Tables **xiii**

1 Introduction **1**
1.1 Background 2
1.2 Objectives and Scope 3
1.3 Outline of the thesis 3

2 Literature review **5**
2.1 Grid impedance estimation 6
2.2 Passive methods 6
2.3 Active methods 8
2.3.1 Transient active methods 8
2.3.2 Steady-state active methods 9

3 HVDC system **11**
3.1 Background 12
3.2 HVDC technologies 12
3.2.1 LCC HVDC 12
3.2.2 VSC HVDC 13
3.3 Converter topologies 13
3.3.1 Two level converter 14
3.3.2 Three level converter 14
3.4 Modular multi-level converter MMC 14
3.5 Control system 14
3.5.1 Upper level controller 15
3.5.2 Lower level control 15
3.5.3 Current controller 16
3.6 HVDC system connected to weak grids 16
3.6.1 Weak AC systems 16
3.6.2 Challenges on HVDC operation with weak HVDC systems . . 16

4 Grid impedance estimation **19**
4.1 Thevenin equivalent Theorem 20
4.2 short circuit capacity 20
4.3 Grid Impedance estimation 21

4.4 Inter-harmonic Signal injection method 21
4.4.1 Inter-harmonic signal generation and injection 22
4.4.2 Inter-harmonic signal measurement and extraction 23
4.5 Online estimation of grid impedance 23
4.6 Impedance calculation technique 23

5 Results and Discussion 25
5.1 Test model description 26
5.2 Estimation evaluation 26
5.3 Test cases 27
5.3.1 Inter-harmonic current with different frequencies 27
5.3.2 Injection in different axes 30
5.3.2.1 d-axis injection 30
5.3.2.2 q-axis injection 31
5.3.2.3 Comparison between d and q axis inter-harmonic current injection 31
5.3.3 Different active power scenario 32
5.3.4 Different reactive power scenario 35
5.3.5 Weak grid case 38
5.3.6 Comparison between inter-harmonic injection different grid impedance estimation technique 40

6 Conclusion and Future work 41
6.1 Conclusion 42
6.2 Future Work 42

Bibliography 43

List of Figures

2.1 The principle of active and reactive power variation - Control system. 7
2.2 The principle of voltage harmonic injection - active and reactive power variations. 7
2.3 PV inverter connected to grid with additional grid impedance measuring unit 8
2.4 Principle of inter-harmonic signal injection 9

3.1 LCC HVDC 13
3.2 VSC HVDC 13
3.3 Simplified schematic of HVDC converter control system 15

4.1 The principle of Thevenin equivalence. 20
4.2 Simplified schematic of the implemented real-time grid impedance estimation technique 22

5.1 CIGRE working group B 4.57 HVDC transmission model 26
5.2 Impedance estimation for different frequencies of the injected inter-harmonic current 28
5.3 Comparison of estimated impedance magnitudes for different inter-harmonic current frequencies 29
5.4 Comparison of estimated impedance angles for different inter-harmonic current frequencies 30
5.5 Impedance estimation for d-axis inter-harmonic current injection . . . 30
5.6 Impedance estimation for q-axis inter-harmonic current injection . . . 31
5.7 Comparison between magnitudes of the estimated impedance for d and q axes injection 31
5.8 Comparison between angles of the estimated impedance for d and q axes injection 32
5.9 Estimated grid impedance magnitude and angle for different active power scenarios 33
5.10 Comparison between magnitudes of the estimated impedance for different active power delivery 35
5.11 Comparison between angles of the estimated impedance for different active power delivery 35
5.12 Estimated grid impedance for different reactive power scenarios . . . 36
5.13 Comparison between the magnitudes of the estimated impedance for different reactive power absorbed by the Ac grid 37

5.14 Comparison between the angles of the estimated impedance for different reactive power absorbed by the Ac grid 38
5.15 Magnitude of the estimated impedance during different active power delivery in a weak Ac grid SCR=1.4 38
5.16 Angle of the estimated impedance during different active power delivery in a weak Ac grid SCR=1.4 39

List of Tables

5.1 Estimated impedance values at the upper side-band frequencies . . . 28
5.2 Corrected impedance values at 50 Hz 29
5.3 Grid impedance estimation error (%) 29
5.4 Estimated grid impedance magnitude at 75 Hz 33
5.5 Corrected impedance estimation magnitude at 50 Hz 34
5.6 Estimated grid impedance angle 34
5.7 Grid impedance estimation error (%) 34
5.8 36
5.9 Grid impedance estimation error (%) 36
5.10 Estimated grid impedance angle 37
5.11 Impedance estimation magnitude at 75 Hz in weak grid case SCR=1.4 39
5.12 Impedance estimation magnitude corrected for 50 Hz in weak grid case SCR=1.4 39
5.13 Grid impedance estimation error in (%) in weak grid case SCR=1.4 . 40
5.14 Comparison between inter-harmonic current injection and RLS algorithm methods 40

1
Introduction

1.1 Background

Electrical power systems are developing more and new technologies are emerging. Conventionally, electric power system activities are classified in to main three main categories: Generation, transmission and distribution.
Generation is the process of converting the energy from variant forms (Thermal, Chemical...etc) in to electrical energy. Recently, new methods of electricity generation have been introduced. Mostly, these new methods use renewable energy sources for electricity generation. The most widely adopted technologies are solar and wind energy sources[8].
In the transmission system, high voltage direct current (HVDC) transmission system is one of the new technologies that are increasing the transmission system capabilities. The possibility to transmit bulk amount of power over long distances became more feasible. Moreover, HVDC technology enables the harvesting of electrical energy from remote energy sources such as, off-shore wind farms and solar fields.
However, HVDC transmission systems encounter some challenges. The connection point of the HVDC for the transmission of RES electricity, can be located far from the large generation plants, leading to a weak grid connection. The efficiency and rated power carrying capacity of direct current transmission lines highly depend on the converter used in transforming the current from one form to another (AC to DC and vice versa). Because of the limitations in the converter, HVDC system operational behavior depends on the AC side grid strength. An enhanced control strategy for achieving a smooth transition between weak and strong AC network is suggested. The concept is based on providing reactive power support to the AC voltage at PCC and exchanging maximum amount of active power within the converter rating limits [16].
Issues regarding performance of an HVDC system connected to a weak AC system are presented. Then an online estimation technique of grid impedance is implanted in PSCAD for a point-to-point HVDC model developed by CIGRE working group B4-57. Effectiveness of the technique during different system's operating conditions is discussed in the results part. Finally, a comparison between the implemented technique and other different technique is also carried out.

1.2 Objectives and Scope

The aim of this thesis work is to apply a grid impedance estimation technique to calculate the grid impedance while the system is running. This is to enhanced the HVDC control system performance by adjusting its parameters according to the AC side system strength.
The first objective of the thesis work is to review different methods and techniques used for online grid impedance estimation. Grid impedance characteristics are key factors in determining the system strength. For different power system areas, the determination of these parameters has different applications. For example, islanding detection, fault location and PV converter control.
The second objective of this thesis work is to select an appropriate method to be used for grid impedance estimation for HVDC applications. The method has to provide reasonable estimation of estimated parameters and within a reasonable time.

1.3 Outline of the thesis

The thesis is organized as follow:
In Chapter 1, an introduction of the thesis work is presented. The aim and scope of the thesis are stated as well.
Chapter 2 is dedicated for the literature review in the thesis topics. The survey encompasses different estimation methods being used and the obtained results. The advantages of each technique and difficulties encountered in each method also presented.
Chapter 3, This chapter is devoted to provide a sufficient background about HVDC systems and their operation, followed by issues with HVDC systems connected to weak AC grids.
In Chapter 4 contains a detailed description of the method implemented in this thesis work. Generation, injection and measurement of the inter-harmonic signal are covered in this chapter.
Chapter 5 , This chapter describes HVDC model used in the simulation. Also, the obtained results are extensively discussed.
Final remarks of the thesis and the future work are presented in chapter 6.

2
Literature review

2.1 Grid impedance estimation

Recently, the accurate determination of the grid impedance characteristics in a power system during system's operation is receiving considerable interest in the research community.
This is because of various applications that requires the impedance parameters' values. These applications spread in different areas such as, HVDC connected to weak ac grids, renewable integration and distributed generation. Also, knowing the grid impedance value allows the identification of potential system's harmonic and resonance problems. Additionally, it can provide a better understanding of the propagation modes for many conducted electromagnetic disturbances, both at harmonic and higher frequencies[17].
In the surveyed literature, there are different techniques that have been used to identify the impedance of different configurations of the Ac grids. The literature mostly covers two main areas where the estimation of the grid impedance was already implemented. These are the distributed energy generation and the photo-voltaic system's integration. However, there is a knowledge gap in the effectiveness of identification of the grid impedance estimation in HVDC applications.
Typically, a dedicated hardware is needed to preform the mathematical calculations for the voltage and current wave-forms in order to obtain the estimated impedance. The most commonly used method for grid impedance estimation have been surveyed. Different methods have been implemented depending on the system's type; Three phase systems and single phase system, for low, medium or high voltage systems.[1]
Assessing the network harmonic impedance is a complex and difficult mission because there is no universal measurement or computational method available. The grid's impedance is continuously changing with loads, network elements and system condition. The state-of-the-art divides the grid impedance estimation techniques into two major categories, the passive and the active methods [2] [5].

2.2 Passive methods

The passive methods make use of the non-characteristic harmonic distortions (voltages and currents) already existed in the system to estimate the grid impedance. In most cases the distortion signals are arbitrary, It has no consistent amplitude nor steady repetition rate to be properly measured [5].
In [6] a non-invasive method (passive method) based on active and reactive power changes was implemented to obtain online estimation of the grid impedance for a single phase system. The authors stated that the method can be used in photo-voltaic systems, small wind turbines and fuel-cells power systems. The implemented method requires PQ control strategy in order to be able to execute the estimation technique. The implemented method is depicted in Figures 2.1 and 2.2 .
The accuracy of this method depends on the PQ variation values (δP - variation value of the active power P and δQ variation value of active power Q) and the duration of the perturbation (δtP - variation power P and δtQ - variation period of reactive power Q).

According to the article, in the passive methods, the output power from the converter is less disturbed comparing to the active methods. The computational complexity is less than other mathematical calculations as DFT and Prony extrapolation.

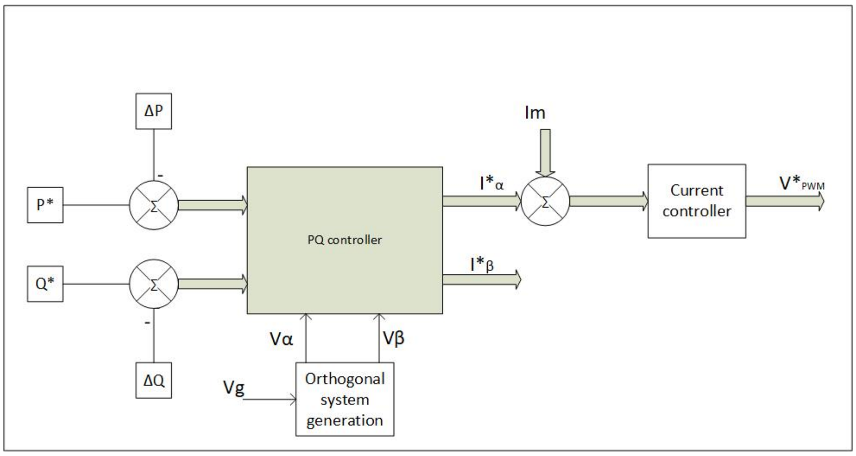

Figure 2.1: The principle of active and reactive power variation - Control system.

Another technique to exploit measurements from the system for impedance estimation is based on grid's voltage and frequency values. A Phase-Looked Loop (PLL) system can be implemented to detect both grid's voltage amplitude and frequency, providing for example the PV system with information about the utility network status[18].

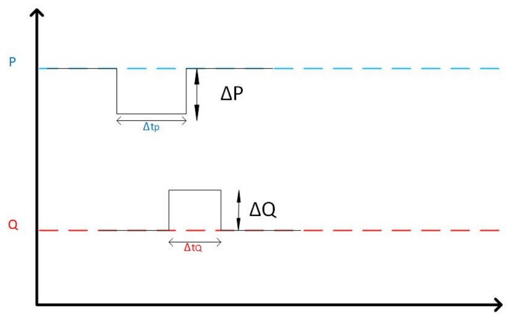

Figure 2.2: The principle of voltage harmonic injection - active and reactive power variations.

Advantages of the passive methods:
1- No disturbance is injected in to the system.
2- The method requires no complicated computational techniques.
There are also some difficulties encountered the implementation of these passive methods:
1- The distortion has neither the amplitude nor the repetition rate to be properly measured.
2- Big measurement errors due to the random nature of the signals.

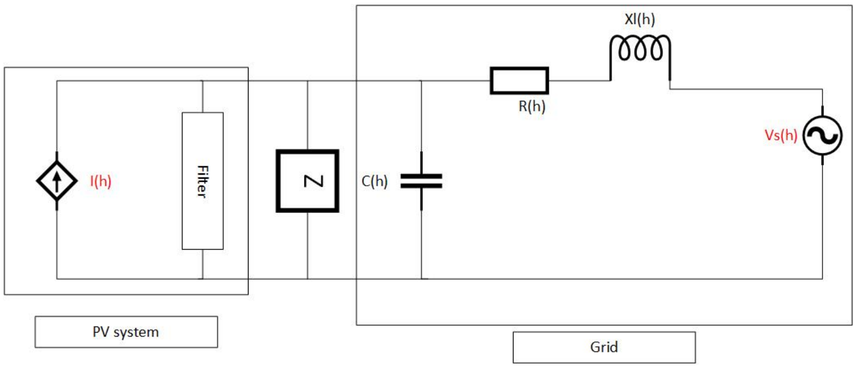

Figure 2.3: PV inverter connected to grid with additional grid impedance measuring unit

2.3 Active methods

In the active methods, a provoked disturbance is injected into the network. Usually, non-characteristic harmonic signal is injected and the response in the system (voltage and current) is measured to obtain the grid impedance parameters. Depending on the characteristic of the injected inter-harmonic signal, the active methods are classified in to two main categories, transient active methods and steady-state active methods.

2.3.1 Transient active methods

Transient active methods are used to obtain fast results because of the short period of the disturbance. First, the inter-harmonic transient current is generated and injected into the grid. Then two measurement values are taken for the voltage and the current at two different instants, before and after impulse injection to estimate the grid impedance parameters.[4]
The main advantage of this method is its ability to estimate the grid impedance over a wide range of frequencies. The impulse will bring in a large harmonic spectrum that afterwards should be analyzed. The measured quantities show the network response over a wide frequency domain, making this method well suited in applications where the impedance is to be observed at different frequencies[5].
In [7], a pulse injection method (PSI) was proposed combined with Luenberger based observer in order to reduce the distortion induced by the excitation signal. This can be done by enabling the observer to trigger the injection mechanism when a change is detected in the grid impedance. It's stated also that the method is suitable for different applications including adaptive control, islanding detection and fault detection.
However, this method may require high performance A/D acquisition devices and must also use special numerical techniques to eliminate noise and random errors.

2.3.2 Steady-state active methods

Steady-state active methods inject a known periodic distortion into the grid during steady state. The response is to be analyzed using Fourier transform or similar methods for the particular injected harmonic to estimate the grid impedance.
There are many techniques to implement these methods. The first technique suggests repetitive connection of a capacitive load to the grid and measuring the phase shift between the voltage and the current. Another method proposes injection of a non-characteristic inter-harmonic current in to the network and record the voltage change response. Most of the reviewed literature suggested steady-state signal injection for grid impedance detection applications [3].
In [6], a periodical injection of one voltage harmonic signal and two voltage harmonic signals were presented. The method is well suited for anti-islanding and robust control of the distributed power generation systems. The use of a higher frequency injection implies an assumption that the grid impedance is linear on this frequency range. However, the estimation error caused by this assumption does not affect significantly the estimation of the grid impedance. The principle of voltage harmonic injection is depicted in figure 2.4. It can be assumed that the respective harmonic is not present in the network. Therefore, the measurements are purely from the inter-harmonic injection response. Also, the parallel capacitor can be eliminated because of its negligible effect at low frequencies.

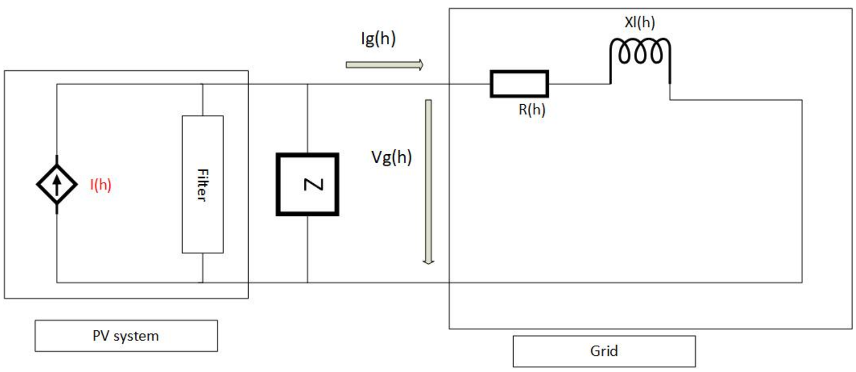

Figure 2.4: Principle of inter-harmonic signal injection

After obtaining Fourier analysis for the measurements, for the specific inter-harmonic signals , the injected harmonic voltage and current can be extracted using notch out filters to eliminate the frequency components in the system. Next, the estimated grid impedance can be calculated as:

$$\underline{Z}(h) = \frac{\underline{V}(h)}{\underline{I}(h)} \tag{2.1}$$

$$\underline{Z}(h) = \frac{V.e^{j\phi_v}}{I.e^{j\phi_i}} = Z.e^{j\phi_Z} \tag{2.2}$$

$$\underline{Z}(h) = R_g + j.2.\pi.f_h.L_g \tag{2.3}$$

where: Z and ϕ_z represent the magnitude and phase angle of the estimated impedance. f_h represents the frequency of the injected inter-harmonic signal.

R_g and L_g (referring to 2.4) denote the resistive and inductive part of the grid; Since the main target is to estimate the grid impedance at the fundamental frequency, further calculation was performed to correct the estimated grid impedance to its corresponding value at the fundamental frequency.

$$\underline{Z}(50Hz) = R_g + j.\omega_{50}.L_g \tag{2.4}$$

The method has the advantage of enabling multiple systems to perform interharmonic injection at the same time and hence, obtaining the grid impedance at multiple points in the grid. Random errors due to noise and A/D flickering can be minimized by controlling the amplitude, duration of the harmonic injection and repetition interval. Because of the aforementioned advantages, this particular method has been selected and implemented in this thesis.

3
HVDC system

3.1 Background

High voltage DC transmission is a power electronic based technology that been implemented in electric power systems for its multiple advantages. High Voltage Direct Current (HVDC) systems have some inherent advantages over AC transmission systems.The efficiency and rated power carrying capacity of the direct current transmission lines are highly depend on the converter used to transform the current from one form to another (AC to DC and vice versa)[8].
Today, there are two main different technologies of HVDC systems. The first type is called LCC HVDC which has multiple applications. It's mainly used in the interconnection within the grid or to connect remote generation plants over long distances. Also, it used as DC links in Ac grids overland or sub-sea, where the conventional AC transmission methods cannot be used. The second one is HVDC VSC also known as HVDC Light within ABB launched in 1997.[11]
The first electrical power transmission system was built in DC, because essentially, electricity was generated from DC generators. However, the major developments in HVDC technologies were in 1950s.[12] The first commercial HVDC was constructed between the Swedish mainland and Gotland island in 1954[11].
The HVDC technologies reached a significant degree of maturity in 1980s. After the considerable development in the power electronics research and industry. The classical HVDC uses thyristor-based current-sourced line commutated converter (LCC) technology. The conventional two-level voltage-source converter (VSC) technology and its variety of configurations resembles the advent of power semiconductor switches in 1980-90s.
The recent emergence of the sub-module based MMC architecture dominates over other converters topologies, due to various technological as well as economic advantages.

3.2 HVDC technologies

High Voltage Direct Current (HVDC) systems have been an alternative method of transmitting electric power from one location to another with some inherent advantages over AC transmission systems. HVDC enabled the transmission of bulk power over long distances. In general, HVDC systems can be classified in several ways; on the basis of cost, flexibility, and operational requirements. A well-configured converter reduces harmonics, increases power transfer capabilities, and reliability. In addition to that, it offers high tolerance to faults along the line.
There are two main HVDC technologies that have been developed, the first is called line commutated converter (LCC), which is thyristor-based converter technology. And the other is called voltage source converter (VSC), which is IGBT based converter technology.

3.2.1 LCC HVDC

The line commutated converters (LCC) are also called current source converters (CSC). The current flows in the power electronic device, the thyristors in this case,

is blocked at the time of switching off the device. This procedure is called "commutation" and the current flows out of the device[9].
The LCC consists of semiconductor elements which has the ability to withstand the voltage in either polarity. Therefore, the current direction remains the same and hence the power direction does not change. LCC has high power capability and less losses per converter (0.7%). However, filters are required due to harmonics generation at low frequencies.

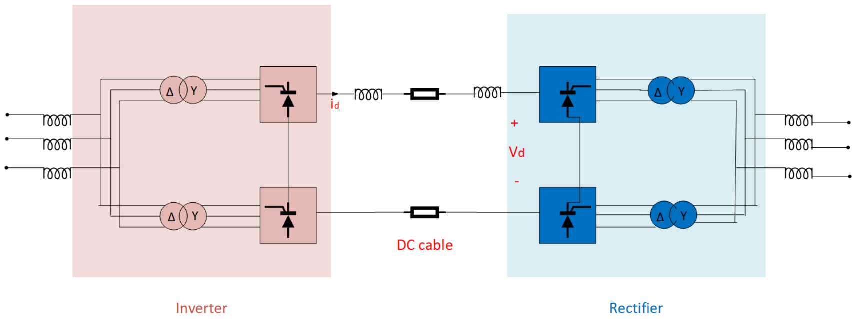

Figure 3.1: LCC HVDC

3.2.2 VSC HVDC

voltage source converters technology is based on IGBTs. Voltage source converters are self commutated converters controlled by the IGBTs switching operation of semiconductor device. The commutation process can take place by self-controlling ON/OFF action of switches of semiconductor devices[9].
The voltage polarity in the DC link remains unchanged.The VSCs have some advantages over current source converters such as much compact size of converter station due to elimination of filters, better controllability. The power flow can be reversed by reversing the current flow.

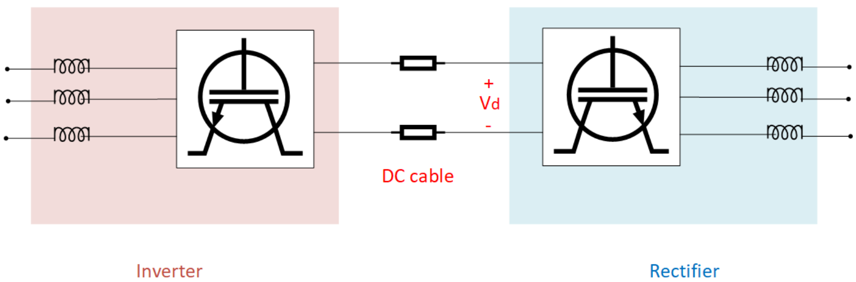

Figure 3.2: VSC HVDC

3.3 Converter topologies

There are different converter topologies in HVDC applications. Two level, three level and MMC are the most commonly used ones. Different switching techniques used resulting in different harmonic level in the output voltage.

3.3.1 Two level converter

Two level converter topology is used in a wide range of power levels. The output voltage is in a square wave form which can be improved by Plus Width Modulation (PWM) technique.
A three phase voltage reference displaced by 120°is provided to the converter.Dominance of higher order harmonics can be avoided by aligning the zero-crossover of each control voltage with zero-crossover of the triangular voltage. Due to the harmonics presented in this topology, multilevel converter topology is introduced to improve the quality of the basic ac wave form[14].

3.3.2 Three level converter

Three level converter is the simplest form of multilevel converter topology. By stepping through several intermediate voltage levels[14].
In multilevel converters, the phase voltage steps are equal to the number of the converter levels (m), while the line voltage has (2m-1) steps. There are two commonly implemented topology concepts in VSC-HVDC, the neutral point clamped (NPC) converters and flying capacitor converters. Modular multilevel converters are introduced to improve the basic ac voltage wave form even further.

3.4 Modular multi-level converter MMC

MMC is a new topology for VSC-HVDC proposed in 2003 at the University of Bundeswehr in Munich, Germany, by Prof. Rainer Marquardt [8].
The proposed topology realizes an approach to improving the waveform and reducing switching losses of two-level or three-level VSC-based HVDC topologies. Multilevel converters provide an output waveform with several voltage levels so that each step in voltage waveform is a fraction of the total voltage swing. Moreover, the switching frequency of each individual power electronics switch is smaller than that of a two-level converter. The voltage step at each level is smaller. These two factors result in a reduced switching loss [15].
In this topology the converter can either adopt the half bridge cascaded or full-bridge connections for the arrangement of each sub modules. The half-bridge modular multilevel (HB-MMC) addresses some of the limitation encountered in the convectional VSC converter. This topology is scalable for the required transmission voltage by just adding more sub-modules. Also, the low-order harmonics are eliminated and the losses reduced to approximately one percent. [8]

3.5 Control system

Normally,an HVDC system operates in constant power control mode.The ordered power (reference power) is given by the operator settings. Reference current then derived from the power controller, which is to be sent to the current controller. The output of the current controller is the provided to the firing control system as a

reference voltage.
In VSC-HVDC active and reactive power can be controlled separately. The inverter side controls the active power, while the rectifier side controls the dc voltage[25]. Different quantities can be controlled in VSC-HVDC, the active power flow, the reactive power flow, the ac voltage, the dc voltage and the frequency. A simplified schematic of HVDC converter control system is depicted in Fig 3.3.

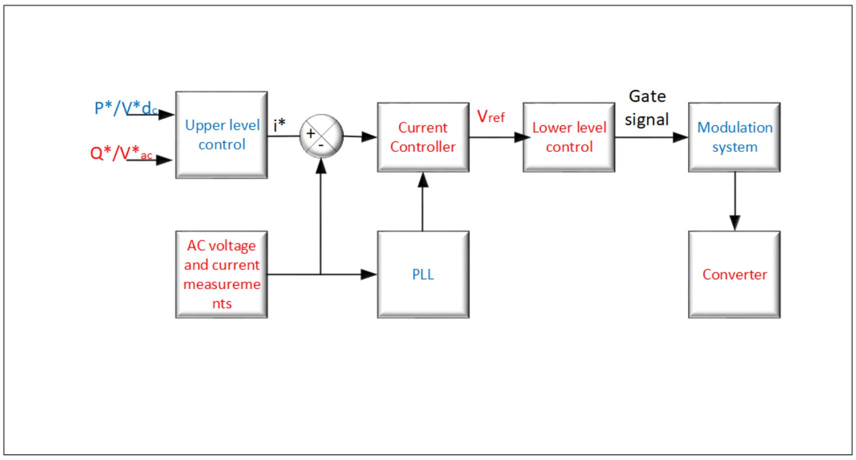

Figure 3.3: Simplified schematic of HVDC converter control system

3.5.1 Upper level controller

This group of controllers can be split into two main categories: reactive power channel and active power channel [3]. The former group comprises a Q-controller and AC voltage controller, whereas the latter includes a P-controller and DC voltage controller.
However, not all the controllers can be used simultaneously. Only one from each category (P/Q power channel) can be used at a given time, depending on the network configuration and the system specifications. A detailed explanation can be found in [15].

3.5.2 Lower level control

The lower level controls comprise circulating current control (CCC) and capacitor balancing control.
In MMC-based VSC-HVDC system, circulating currents originate from the phase difference between the MMC legs or within the upper or lower arm itself due to the difference capacitor voltage in the sub-modules. It consists of DC and AC part. The DC part is responsible from the active power delivery out of the converter.The AC part is to provide reactive power flow among the MMC legs. However, it leads to decreasing the efficiency of the MMC. Thus, it must be suppressed.
The aim of the capacitor balancing control is to charge the submodules with the lowest capacitor voltages and on the other side, discharge the submodules with the highest capacitor voltages depending on the arm current direction.

3.5.3 Current controller

The current controller aim to provide a reference voltage (V_{ref}) for the lower level control in order to control the active and reactive power at the point of common coupling.
Normally, current controller is implemented in the dq reference frame with two reference currents i_d and i_q as inputs to the current controllers. In this thesis work an inter-harmonic current is injected to either the d or q reference currents. equations 3.1 and 3.2 depict the ac current dynamics and the current controller design respectively.

$$V_{abc} = L\frac{di_{abc}}{dt} + Ri_{abc} \tag{3.1}$$

The current controller with voltage feedforward and cancellation of the dq cross coupling terms is designed as,

$$V_{ref} = -(K_p + \frac{K_i}{S})(i_{ref} - i) - jw_1 Li + \frac{\alpha_c}{S + \alpha_c}E \tag{3.2}$$

Where,
V_{ref} is the output of the current controller.
E is the controlled ac voltage[25].

3.6 HVDC system connected to weak grids

3.6.1 Weak AC systems

The ability of an AC network to restore its normal operational behavior after disturbance implies its strength. This strength depends on grid's impedance and inertia. The stronger the grid, the smaller the impedance is, resulting in fast recovery of the system voltage after disturbances. Also, grids with bigger inertia restore its synchronous speed and hence the frequency faster. The system's strength is expressed as an absolute numerical value termed Short Sircuit Ratio(SCR). The Short Circuit Ratio (SCR) is defined as the ratio of system's short circuit level (MVA) to the dc power (MW), has been used to indicate system strength.[10]

3.6.2 Challenges on HVDC operation with weak HVDC systems

Power systems are the largest man-made systems in existence and the most complex ones. Planning, operation and control of power systems require extensive mathematical methods to solve the problems that encountered during theses processes.
Usually, electrical power systems consist of large number of transmission lines connected in a fashion that is dictated by the development of load centers. Faults of different types may occur in the system. Therefore, the configuration of the system changes during its operation.[4]

If the a wind farm is to be connected to the main grid via a long transmission line, this leads to a high line impedance and hence, weak grid connection. The IEEE transmission and distribution committee used short-circuit ratio (SCR) to describe grid's strength and defined weak grid as of ($SCR < 3$). However, systems with ($SCR < 1.2$) are considered extremely, weak systems[23]. Dynamics of control system in grid-connected VSC become more complicated when connected to a weak ac grid and often stability becomes a major concern. The change in the grid impedance could possibly yields in a change in its strength level. For example, from moderately strong grid ($3 \geq SCR \geq 2$) to weak grid ($SCR \leq 2$) which affects the stability of the control system. Therefore, an online change of the converter controller parameters or change in the control mode enhances the performance of the control system of the converter[23].

4
Grid impedance estimation

4.1 Thevenin equivalent Theorem

The Thevenin theorem (Thevenin equivalent circuit) is one of the fundamental theories in electrical circuits analysis. The theorem states that an entire electrical circuit can be replaced by a voltage source in series with an equivalent impedance.
In other words, According to the Thevenin's theorem, the electrical grid can be represented by an ideal voltage source behind an impedance[20] [21].

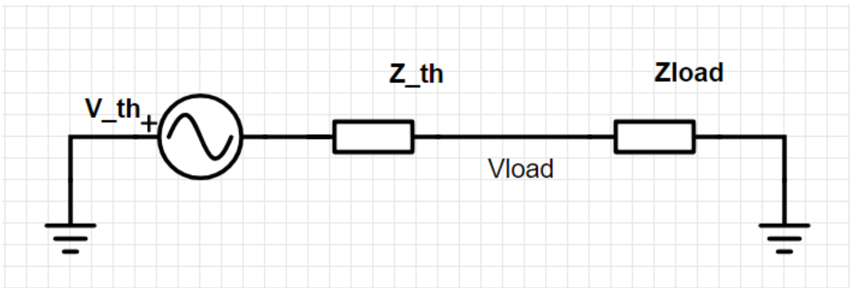

Figure 4.1: The principle of Thevenin equivalence.

The voltage at the point of load connection is always lower than E_{th} because of the voltage drop across the equivalent Thevenin impedance Z_{th}. However, if the Thevenin's impedance Z_{th} becomes smaller, then the load voltage V_l becomes closer to E_{th}. Ideally, if Z_{th} is zero, then the load voltage V_l is exactly the same as E_{th} .

$$V_l = E_{th} - I.Z_{th} \tag{4.1}$$

Z_{th} is also called the short circuit impedance of the grid. This is because when the grid is directly short circuited to the ground, Z_{th} is the only impedance between the Thevenin voltage source E_{th} and the ground. Figure 4.1 depicts the concept of Thevenin equivalence theorem.
For simplicity, the impedance of the ac grid connected to an HVDC system is reduced to its equivalent Thevenin impedance Z_{th} to Study the the between the two systems.

4.2 short circuit capacity

The apparent power absorbed from the grid during short circuit is called the short circuit capacity(SCC) of this grid. SCC in MVA is defined as

$$SCC = E_g^2/Z_g \tag{4.2}$$

Wheres,
$|E_{th}|$ denotes the rated voltage of the grid.
Z_g denotes the equivalent grid impedance.
The electrical grid is considered to be strong grid when it has a high SCC (or a smaller Z_{th}). In contrast, the grid is weak if it has a lower SCC (or a bigger Z_{th}). Ideally, the grid has an infinite SCC when Z_{th} is zero. This is the strongest grid. In this case, $V_l = E_{th}$.

The Short Circuit Ratio (SCR) measures the system strength in most cases, which is the ratio of the Short-Circuit capacity (SCC) to dc link power (P_{dc}) at the injection point.

$$SCR = SCC/P_{dc} \tag{4.3}$$

The SCR, from the impedance point of view, is a measure of how high is the bus impedance for that grid node. It has been considered that an AC system is strong when $SCR \geq 3$, weak when $2 \leq SCR < 3$ and very weak when $SCR < 2$ [16].

4.3 Grid Impedance estimation

Electric power systems are designed to operate continuously delivering the power from the generation plants to the load centers. During its operation, a power system experiences different events and incidents which might change the grid configuration. A change in grid configuration results in a corresponding change in the equivalent grid impedance seen from specific point (node) in the system. For example, if one of two parallel transmission lines tripped, the total equivalent impedance of the grid seen at any point changes.
The grid impedance value is a crucial factor in power systems studies. For instance, if plans have been made to install a new component or more in the grid, pre-installation studies require the knowledge of the grid impedance in order to study the overall system performance after having the new equipment installed.
In this case, the behavior of the HVDC system is depending on the strength or weakness of the AC system it's connected to. The overall converter performance and stability vary with the strength of the AC system. The transmitted power is exposed to power transmission limitations that have been imposed on a VSC-HVDC converter by the ac system strength.
There are different methods to calculate the grid impedance online. The complete review of these methods has been presented in the literature review of this report. For this thesis work, the steady-state inter-harmonic signal injection of the active methods has been selected to perform the estimation, because of its advantages and suitability to the investigated system.

4.4 Inter-harmonic Signal injection method

The steady-state inter-harmonic signal injection method is implemented to calculate the grid impedance during the system's operation.
The concept behind this method is to inject an inter-harmonic signal (voltage or current) into the AC side system from the point of common coupling (PCC) and measure the system response in the (voltage or current) signal. Then impedance is calculated from the measured voltage and current values. An observer can be implemented to trigger the estimation algorithm after detection of abnormal condition in the system. This is to reduce the disturbance time to secure system stability and reduce THD in the system.
The amplitude, frequency and duration of the injected inter-harmonic signal should

be selected in order to have accurate and fast impedance estimation. Also, to reduce the disturbance introduced to the system. Figure 4.2 illustrates the implemented grid impedance estimation technique.

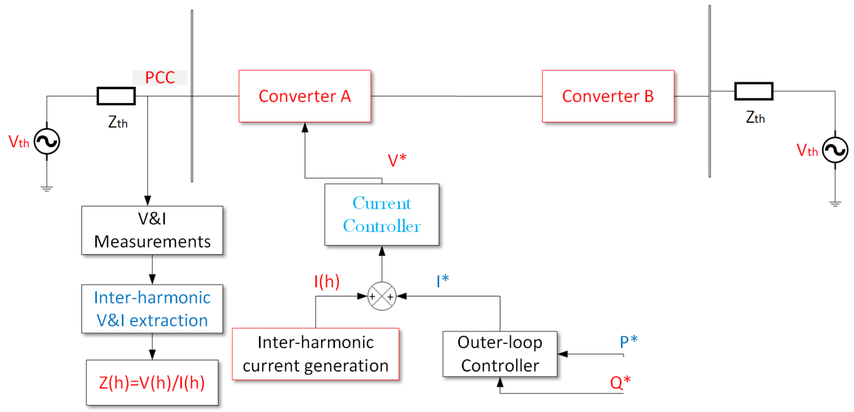

Figure 4.2: Simplified schematic of the implemented real-time grid impedance estimation technique

4.4.1 Inter-harmonic signal generation and injection

A simulation setup with a point-to-point HVDC link based on CIGRE working group B4.57 is implemented in PSCAD. An inter-harmonic signal is generated and injected through the HVDC converter into the AC side system and the response in measured.
Initially, the signal is generated as a sinusoidal inter-harmonic current with an amplitude of small percentages of the rated current.This value is selected to be as minimum as possible in order to reduce the the disturbance provoked in the system. However, it should be big enough to be extracted by the filters after the measurement. The frequency of the inter-harmonic current is chosen to be as close as possible to the fundamental frequency in order to maximize the accuracy of the estimation.
The inter-harmonic current is selected to be of a sub-synchronous frequency (f_{in}) and to be added to either the d or q current references in the synchronous reference frame. The signal is therefore to be extracted at ($50\pm f_{in}$). These are called the upper and the lower side-bands. The duration of the injection (d_{in}) is decided to be of few hundreds of milliseconds in order to reduce the THD in the current waveform. The injection is to be triggered by a signal from observer after a change detection in the system configuration. Due to valve current limitations, it's safer to inject known inter-harmonic current signal and measure the response in the voltage wave-form. Current controller gives output voltage reference, which has the inter-harmonic component embedded in to it, to the modulation technique. In other words, the output signal at the converter's terminal is combining the inter-harmonic voltage signal injected to the AC system.

4.4.2 Inter-harmonic signal measurement and extraction

After embedding the inter-harmonic signal to the reference voltage, which is generated at the converter terminals, voltage and current are measured at the point of common coupling (PCC).
An extraction algorithm fro the injected inter-harmonic current signal and the corresponding voltage is implemented. Since, the inter-harmonic current signal is added to the reference current in the synchronous reference frame (dq- reference frame), these quantities reflect at ($f_i n \pm 50$) in the three phase system due to the transformation from the synchronous frame components to the three phase system.
The first step is to eliminate the fundamental component using a notch filter with characteristic frequency of 50Hz. Then the measured signal is passed through a band pass filter to allow only the specific inter-harmonic current component to be in the output. The same procedure goes to the voltage wave-form.
A careful tuning of the extraction algorithm filters is needed in order not to affect the measured signal. A compensation for the gain reduction imposed by the filters is also necessary.

4.5 Online estimation of grid impedance

The grid impedance can be easily calculated for any specific grid configuration. However, during system operation different events occur in the system might lead to changes in the system configuration, and hence the grid impedance.
The process of calculating the grid impedance during operation is not handy, because imposing changes during system running might affect system performance and stability. Therefore, the active method implementation based on the injected inter-harmonic current has to be carefully designed. This can be done by carefully, select the characteristics of the injected inter-harmonic signal. It's magnitude, frequency and duration of injection. The overall system performance during signal injection is to be observed and analyzed for any possible violations in the system performance.

4.6 Impedance calculation technique

Having the specific inter-harmonic voltage and current signals been extracted, the impedance calculation algorithm based on Ohm's law of voltage and current division is implemented. A simple trigonometric equations is implemented to calculate the impedance characteristics (real and imaginary) parts of the complex impedance using single phase quantities.
Two cascaded filters are used to obtain 90° phase shift of the measured inter-harmonic voltage and current signals. Equations 4.5 and 4.6 are used to calculate the real and imaginary parts of the estimated impedance.
The time constant for the implemented filters is:

$$T_f = \frac{1}{2\pi f_h} \tag{4.4}$$

Then the real and imaginary parts of the impedance is calculated as follows:

$$Z_{re} = \frac{v * sin(\alpha_v) i * sin(\beta_i) + v * cos(\alpha_v) i * sin(\beta_i)}{i^2} \tag{4.5}$$

$$Z_{img} = \frac{v * cos(\alpha_v) i * sin(\beta_i) + v * sin(\alpha_v) i * sin(\beta_i)}{i^2} \tag{4.6}$$

Then the magnitude and phase angle of the estimated impedance is obtained as:

$$|Z| = \sqrt{Z_{re}^2 + Z_{img}^2} \tag{4.7}$$

$$\phi_z = \arctan(\frac{Z_{img}}{Z_{re}}) \tag{4.8}$$

By providing both signals 90° phase shift the real and imaginary parts of the complex impedance can be calculated directly.
The magnitude and the angle of the estimated impedance can be obtained from the calculated reals and imaginary parts.

5

Results and Discussion

5.1 Test model description

A benchmark Model developed by CIGRE working group B4-57 was used to implement the selected grid impedance estimation technique. Some modifications have been realized in the model to implement the estimation technique.
A grid with known impedance was built in order to compare the estimated impedance parameters with the actual impedance values. Also, an inter-harmonic generation circuit was implemented to generate the inter-harmonic current in order to be injected into the grid. Figure 5.1 shows a general overview of the model used to implement the selected estimation technique.
The model used consists of a point-to-point HVDC transmission system connecting two AC grids at the terminals. The first grid is considered to be an extremely strong grid. While the parameters of the other grid are modified to a known impedance parameters and short circuit ratio (SCR). The estimation technique was conducted for the modified grid.
The converters technology is voltage source converter (VSC), having a topology of a half bridge modular multilevel converter (MMC) in a symmetric monopolar configuration (± 400Kv), each pole connected through 150 Km cable. Each converter is composed of 6 arms with two arms for each phase, having 350 cells per arm. Base power is 1265 MVA.
The control system comprises of three main levels; The upper control level, the lower control level and the converter control. The dispatch operator's commands are the input to the upper level control, while, it provides reference voltage signal to the lower level control. The inter-harmonic current signal is to be injected to the reference i_d or i_q current in the upper level control. In figure **??**, the complete procedure of the estimation technique is depicted.

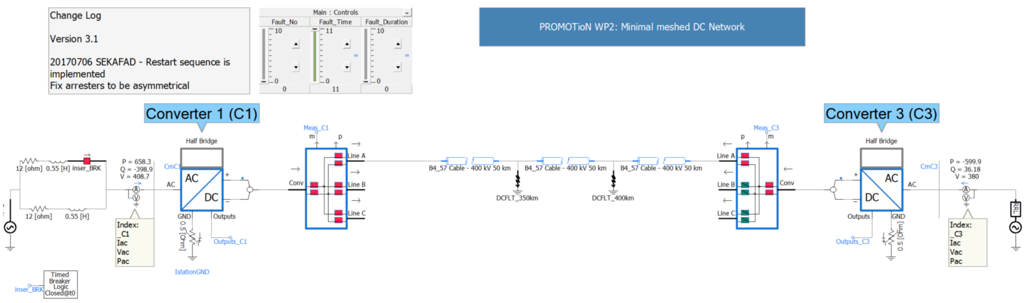

Figure 5.1: CIGRE working group B 4.57 HVDC transmission model

5.2 Estimation evaluation

To evaluate the estimation accuracy, the estimated impedance parameters were compared with the actual impedance values.
The estimation time (t_{es}) is the time from the injection initiation to the time that the estimation converges within specific estimation error, for specific inter-harmonic injection. Also the estimation time is a key factor in this estimation technique performance evaluation.

5.3 Test cases

To evaluate the performance of the estimation technique, results from different operational conditions of the system were discussed.
Simulations have been executed to estimate grid impedance parameters during different system operational conditions. The generated inter-harmonic current signal is then added to either of the reference current components in the synchronous reference frame(i.e. i_d or i_q). Then the corresponding voltage and current inter-harmonic signals were extracted at upper side-band (at 75 Hz) due to transformation since it gives better estimation than the lower side-band.
The characteristics of the injected inter-harmonic signal are; the amplitude is 0.0091p.u. corresponds to (1%) of the nominal current. The frequency of the injected signal and duration its duration are specified in the following simulations.

5.3.1 Inter-harmonic current with different frequencies

In this case an inter-harmonic current with different frequencies each time was injected to estimate the grid impedance. The actual grid impedance at the fundamental frequency (f = 50Hz) is $Z = 2 + j40$ Ohm, The amplitude = 40.05 Ohm and θ = 87°. The test was performed in a strong grid with short circuit ratio (SCR) = 3. The estimation error observed is as depicted in table 5.1.

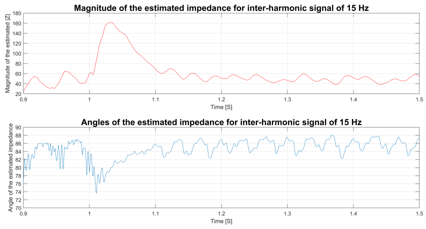

(a) 15 Hz inter-harmonic current injection

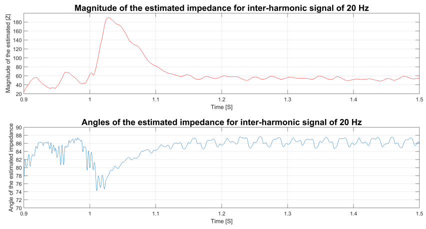

(b) 20 Hz inter-harmonic current injection

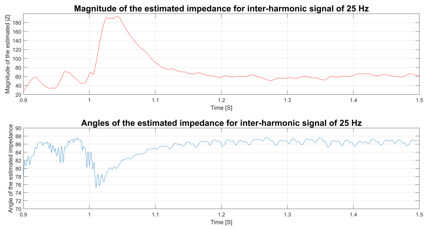

(c) 25 Hz inter-harmonic current injection

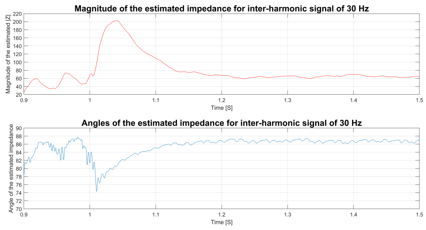

(d) 30 Hz inter-harmonic current injection

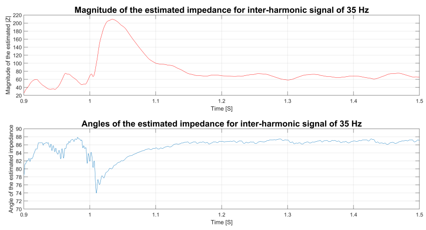

(e) 35 Hz inter-harmonic current injection

Figure 5.2: Impedance estimation for different frequencies of the injected inter-harmonic current

Figure 5.2 shows magnitude and angle of the estimated grid impedance for different frequencies 15Hz, 20Hz, 25Hz and 30Hz consecutively.
The convergence of the estimated impedance parameters are dependent on the frequency of the injected inter-harmonic current. The oscillations in the estimated impedance is inversely proportional to the frequency of the injected inter-harmonic signal.

Frequency	|Z| at 100 ms	|Z| at 200 ms
15 Hz	68.6	50.2
20 Hz	81.8	59
25 Hz	90.94	59.54
30 Hz	109.3	67.39
35 Hz	99.89	68.81

Table 5.1: Estimated impedance values at the upper side-band frequencies

Frequency	|Z| at 100 ms	|Z| at 200 ms
15 Hz	45.7	33.47
20 Hz	54.53	39.33
25 Hz	60.63	39.69
30 Hz	72.87	44.93
35 Hz	66.59	45.87

Table 5.2: Corrected impedance values at 50 Hz

Table 5.3 depicts the grid impedance estimation error at two different points of time after inter-harmonic signal injection.
These tests reveal that 25 Hz is the frequency which yields the least impedance estimation error (-0.775% at 200ms). The fine tuning of inter-harmonic extraction filters results in better operation of the estimation technique. The upper side-band frequencies have always better estimation performance than the lower side-band frequencies. Therefore, only the upper side-band frequencies are considered for this purpose.

Frequency	estimation error(%) at 100 ms	estimation error (%) at 200 ms
15 Hz	14.25	-16.325
20 Hz	36.325	-1.675
25 Hz	51.575	-0.775
30 Hz	82.175	12.325
35 Hz	66.475	14.675

Table 5.3: Grid impedance estimation error (%)

In figure 5.3 a comparison between magnitude of the estimated impedance for different inter-harmonic current frequencies is presented. While Figure 5.4 the same comparison is done for for the estimated angle.

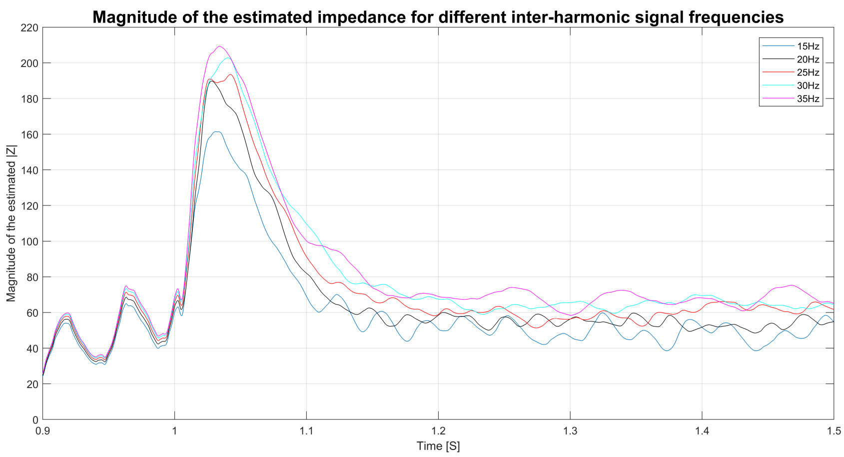

Figure 5.3: Comparison of estimated impedance magnitudes for different inter-harmonic current frequencies

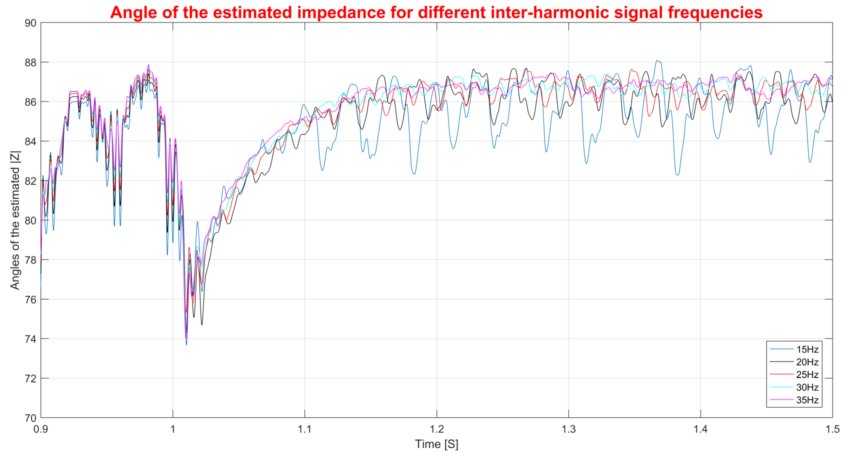

Figure 5.4: Comparison of estimated impedance angles for different inter-harmonic current frequencies

5.3.2 Injection in different axes

5.3.2.1 d-axis injection

In this case, an inter-harmonic current component is added to the d-axis reference current. Initially, the estimated impedance rises to a higher value during injection transient, then after the measurement settles in steady state value, calculated value of impedance can be selected.
Given the system status in this case, transmitted active power = 600 MW, Q= 0 MVAr, i_h=0.0091 p.u., F_h=25Hz. Inter-harmonic current signal is injected at 3s, the estimated impedance magnitude is 45.5 and 38.5 with estimation error of 13.75% and -3.75% after 150 ms and 200 ms respectively. the negative sign denotes underestimation of the grid impedance. Estimated impedance angle was 86.6°and 86.4°after 150 ms and 200 ms from the injection initiation respectively.

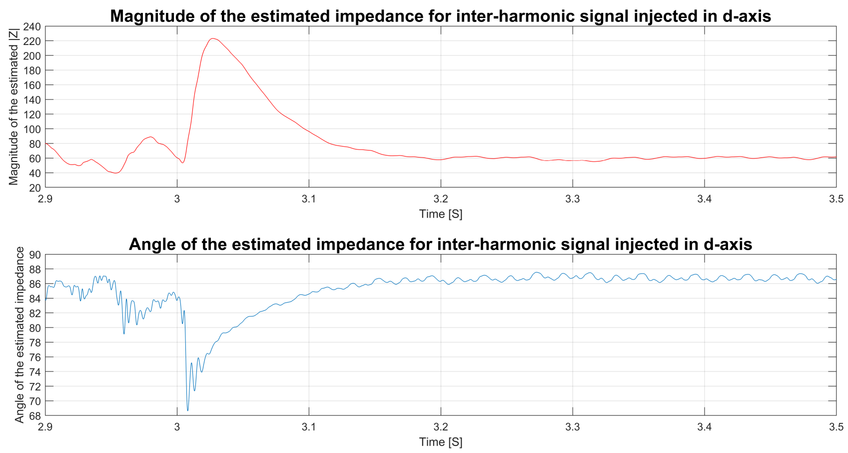

Figure 5.5: Impedance estimation for d-axis inter-harmonic current injection

5.3.2.2 q-axis injection

Similarly, as in the previous case, the same inter-harmonic current is now added to the reference q current instead. Estimated grid impedance magnitude is 48.5 and 40 resulting in an error of 21.3% and 0% at 150 ms and 200 ms respectively. On the other hand the estimated impedance angle was 86.5°and 86.7°respectively.

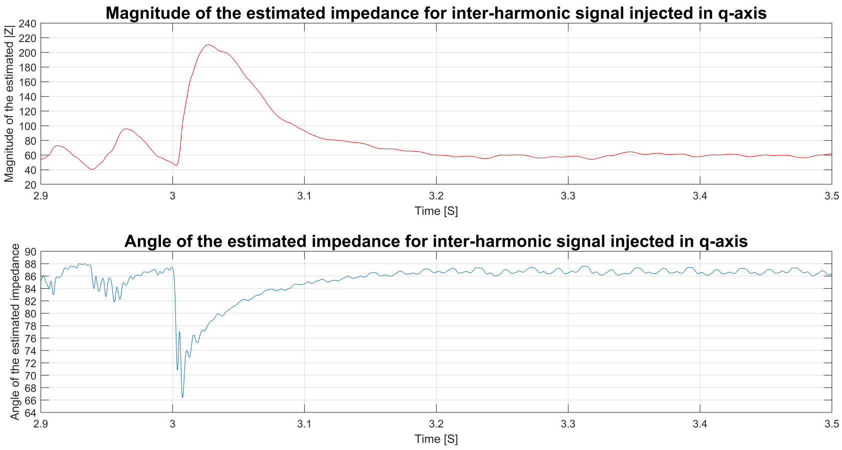

Figure 5.6: Impedance estimation for q-axis inter-harmonic current injection

5.3.2.3 Comparison between d and q axis inter-harmonic current injection

Figures 5.7 and 5.8 show grid impedance magnitude and angle estimation for the same injected inter-harmonic current, it can be observed that injection in the q-axis gives slightly better estimation specially, if there is no reactive power injected or absorbed by the converter.

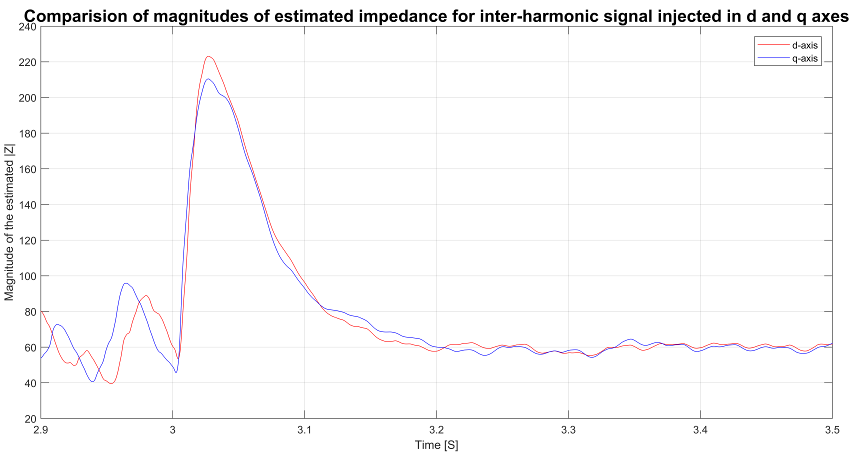

Figure 5.7: Comparison between magnitudes of the estimated impedance for d and q axes injection

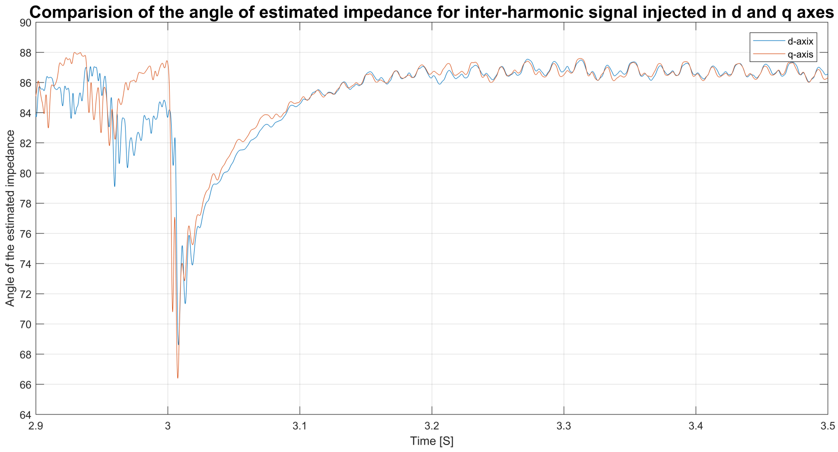

Figure 5.8: Comparison between angles of the estimated impedance for d and q axes injection

5.3.3 Different active power scenario

In this case, the performance of the impedance estimation technique under different active power transmitted over the HVDC system was investigated.
The following tables 5.4 and 5.5 show the impedance estimation during different loading conditions.

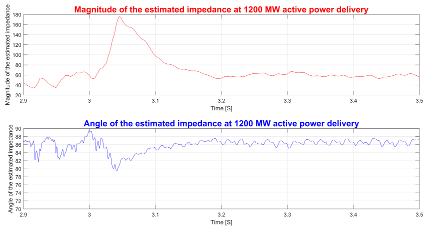

(a) Amplitude of the estimated impedance at 1200 MW

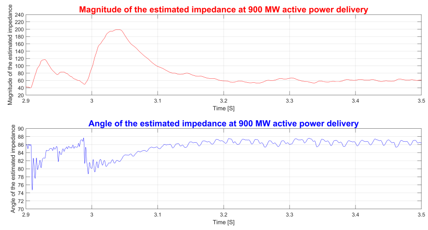

(b) Amplitude of the estimated impedance at 900 MW

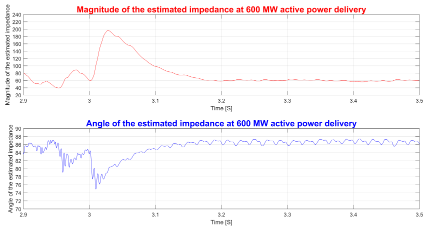

(c) Amplitude of the estimated power during 960 MW

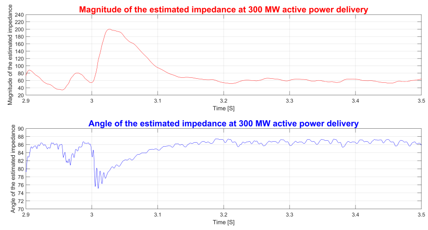

(d) Amplitude of the estimated power during 300 MW

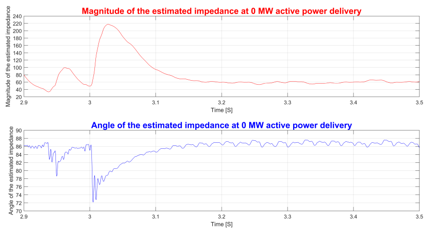

(e) Amplitude of the estimated power during 0 MW

Figure 5.9: Estimated grid impedance magnitude and angle for different active power scenarios

Transmitted power	impedance estimation at 150 ms	impedance estimation at 200 ms
0 MW	70.8	56.8
300 MW	70.6	59.8
600 MW	72.3	58
900 MW	69.2	54
1200 MW	69.2	54.1

Table 5.4: Estimated grid impedance magnitude at 75 Hz

Transmitted power	impedance estimation at 150 ms	impedance estimation at 200 ms
0 MW	47.2	37.9
300 MW	50.4	39.9
600 MW	48.2	38.7
900 MW	46.1	36
1200 MW	46.1	36.1

Table 5.5: Corrected impedance estimation magnitude at 50 Hz

Transmitted power	impedance angle at 150 ms	impedance angle at 200 ms
0 MW	86.7	86.6
300 MW	86.5	86.9
600 MW	86.6	86.3
900 MW	86.7	86.7
1200 MW	86.6	86.2

Table 5.6: Estimated grid impedance angle

Table 5.7 demonstrates the error in the estimation of the grid impedance magnitude at two instants after injection of the inter-harmonic signal injection. After 200 ms, the estimation error is less than 10% in all the simulated cases. This time can be considered as the estimation time in the worst case scenario for such tolerance in the estimation.
Generally, the estimation result is a trade-off between estimation time and accuracy. For such HVDC application, the estimation time is favored over estimation accuracy due to the sensitivity of the system to the HVDC transmission system because of the bulk power been transmitted over HVDC transmission systems.

Transmitted power	estimation error at 150 ms (%)	estimation error at 200 ms (%)
0 MW	18	-5.3
300 MW	26	-0.3
600 MW	20.5	-3.3
900 MW	15.3	10
1200 MW	15.3	-9.8

Table 5.7: Grid impedance estimation error (%)

Figures 5.10 and 5.11 show comparison between magnitudes and angles of the estimated impedance at different power delivery.

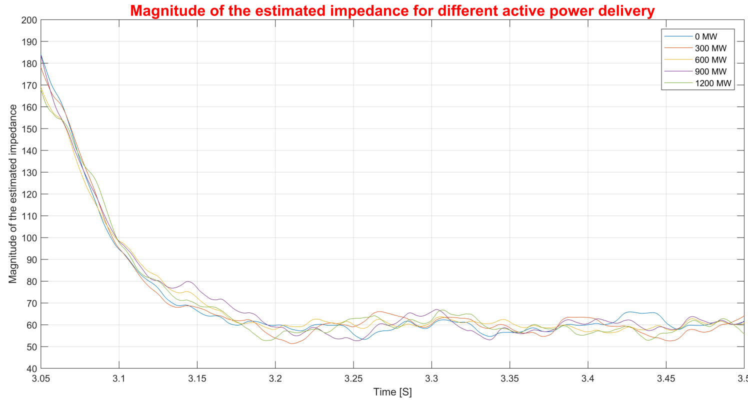

Figure 5.10: Comparison between magnitudes of the estimated impedance for different active power delivery

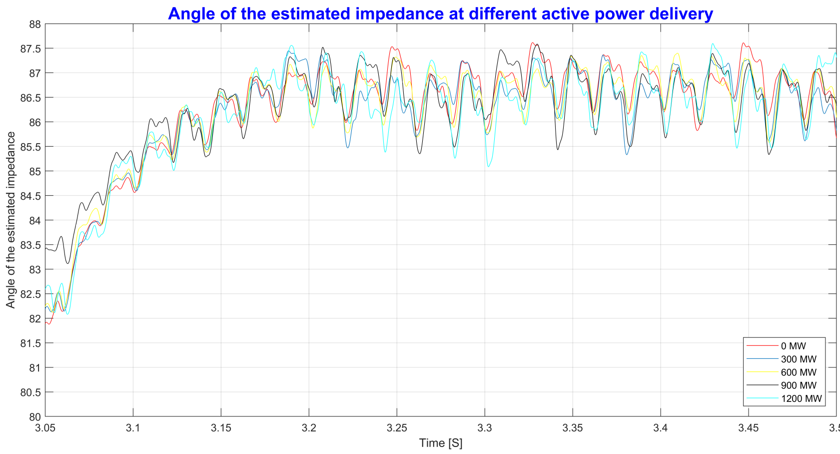

Figure 5.11: Comparison between angles of the estimated impedance for different active power delivery

5.3.4 Different reactive power scenario

In this simulation, the inter-harmonic current is injected in q axis because it's the reactive current axis. The reactive power is generated from the converter and injected to the ac grid. Figures 5.12 depicts the convergence of the estimated impedance magnitude and angle for different converter reactive power generation operation conditions.

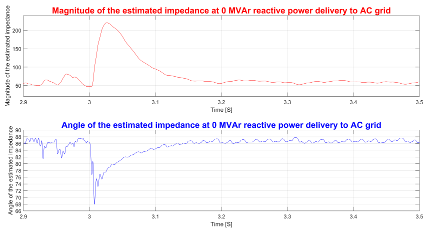

(a) Magnitude and angle of the estimated impedance during 0 MVAr produced by the converter

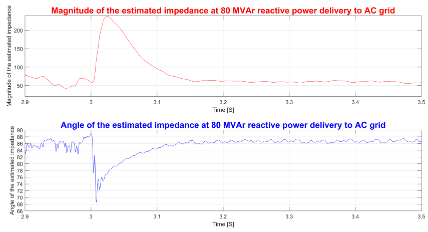

(b) Magnitude and angle of the estimated power during 80 MVAr produced by the converter

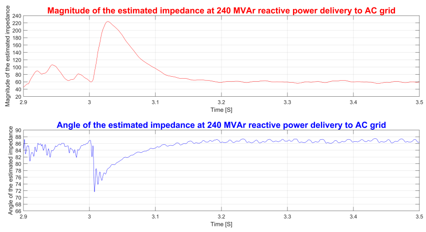

(c) Magnitude and angle of the estimated power during 240 MVAr produced by the converter

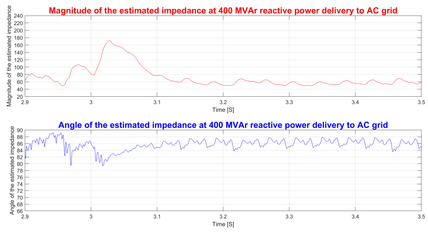

(d) Magnitude and angle of the estimated power during 400 MVAr produced by the converter

Figure 5.12: Estimated grid impedance for different reactive power scenarios

Reactive power	Z_{es} estimation at 150 ms	Z_{es} estimation at 200 ms
0 MVAr	65.9	55.8
80 MVAr	63.3	61.6
240 MVAr	67.2	58.5
400 MVAr	65.2	50.8

(a) Impedance estimation magnitude at 75 Hz

Reactive power	Z_{es} estimation at 150 ms	Z_{es} estimation at 200 ms
0 MVAr	43.9	37.2
80 MVAr	42.2	41.1
240 MVAr	44.8	39
400 MVAr	43.5	33.9

(b) Corrected impedance estimation magnitude at 50 Hz

Table 5.8

Reactive power	Estimation error(%) at 150 ms	Estimation error(%) at 200 ms
0 MVAr	9.8	-7
80 MVAr	5.5	2.8
240 MVAr	12	-2.5
400 MVAr	8.8	-15.3

Table 5.9: Grid impedance estimation error (%)

Table **??** shows values of the magnitude of the estimated impedance extracted for measured quantities at 75 Hz. while table 5.8 shows the magnitude of the linearly corrected impedance to the fundamental frequency (50 Hz). Table 5.10 depicts the estimated impedance angle for different reactive power injected to the Ac system. In table **??**, impedance estimation error is presented.

Reactive power	impedance angle at 100 ms	impedance angle at 200 ms
0 MVAr	86.8	86.2
80 MVAr	86.8	86.4
240 MVAr	86.6	86.3
400 MVAr	87.5	87

Table 5.10: Estimated grid impedance angle

In figures 5.13 and 5.14 a comparison between the magnitudes and angles of the estimated impedance for different reactive power generation by the converter is shown.

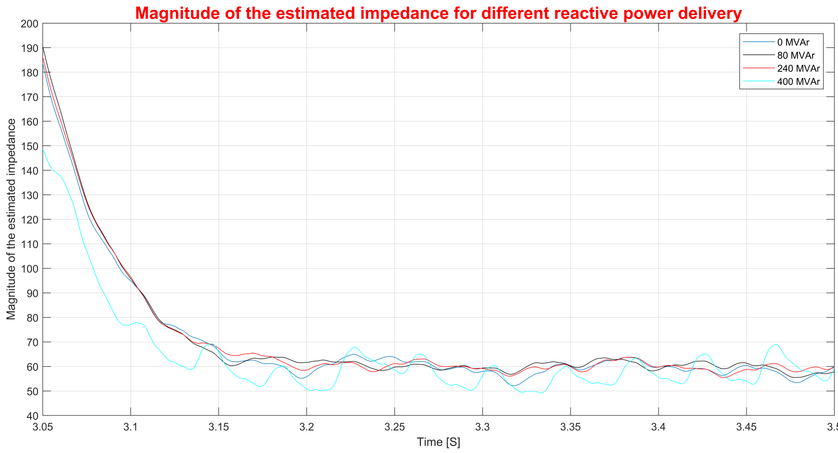

Figure 5.13: Comparison between the magnitudes of the estimated impedance for different reactive power absorbed by the Ac grid

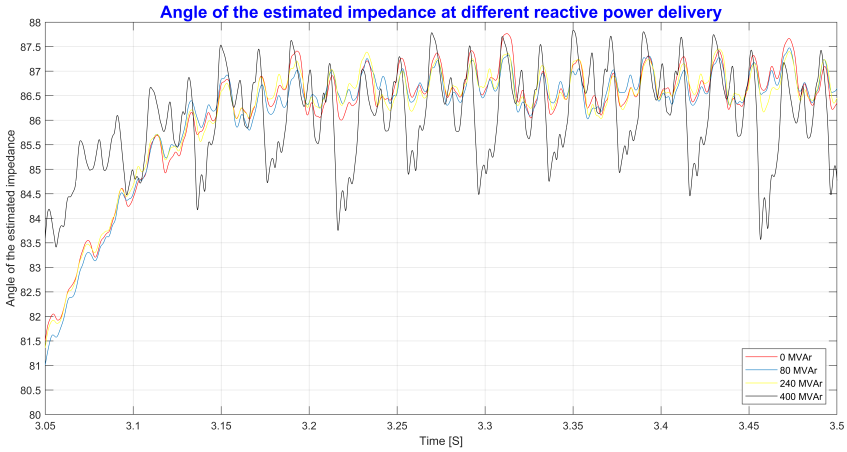

Figure 5.14: Comparison between the angles of the estimated impedance for different reactive power absorbed by the Ac grid

It can be observed from table 5.9 that the estimation technique has an error less than 10% at 200 ms after injection initiation except for the last case of 400 MVAr reactive power being injected into the ac grid because of the oscillatory reactive power in the model. In addition to that, the estimated impedance angle also has more oscillations in the 400 MVAr scenario because of the same reason.

5.3.5 Weak grid case

In this scenario, a weak ac grid with a Short Circuit Ratio (SCR) of 1.4 was implemented to evaluate the performance of the estimation technique. The actual impedance of the grid $Z = 6 + j86.4$ Ohm, $|Z| = 86.6$ Ohm and $Z_{phi} = 86.03°$. By having the converter works in Ac voltage control mode, the following results in figures 5.15 and 5.16 show a comparison between the magnitude of the estimated grid impedance during different active power delivery. Also, the the estimation of the impedance angle during the same active power delivery is presented to asses the performance of this estimation technique.

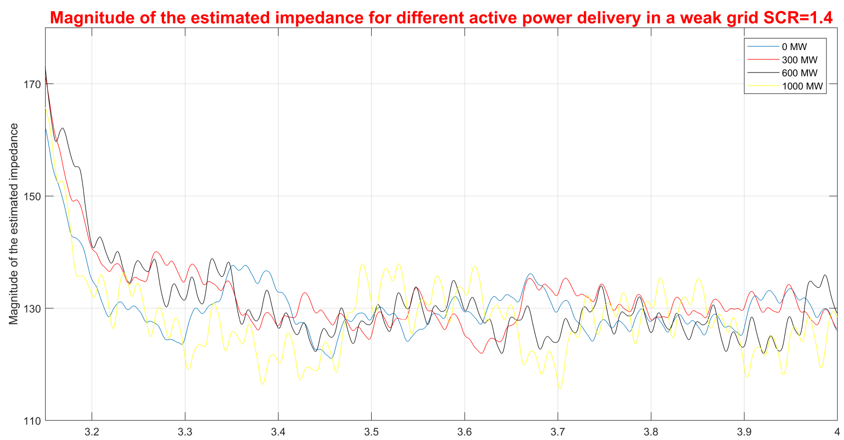

Figure 5.15: Magnitude of the estimated impedance during different active power delivery in a weak Ac grid SCR=1.4

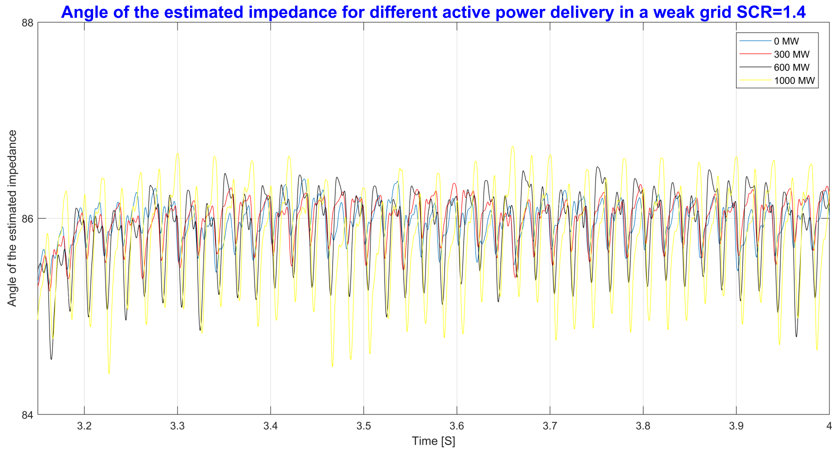

Figure 5.16: Angle of the estimated impedance during different active power delivery in a weak Ac grid SCR=1.4

Reactive power	impedance estimation at 150 ms	impedance estimation at 200 ms
0 MW	161.6	135.1
300 MW	170.6	140.6
600 MW	171.7	148.7
1000 MW	171.5	141.2

Table 5.11: Impedance estimation magnitude at 75 Hz in weak grid case SCR=1.4

Reactive power	impedance estimation at 150 ms	impedance estimation at 200 ms
0 MW	107.7	90
300 MW	113.7	93.7
600 MW	114.5	99.1
1000 MW	114.3	94.1

Table 5.12: Impedance estimation magnitude corrected for 50 Hz in weak grid case SCR=1.4

Generally, it can be observed that the impedance estimation errors were higher in this weak grid case. Figure 5.15 shows the estimated impedance magnitude of the weak AC grid at different HVDC transmission system loading cases. Table 5.11 shows the output grid impedance estimation from the estimation technique at the upper side-band (75Hz). These values were then corrected for 50Hz in table 5.12 by applying a simple linear correction method to the obtained estimated impedance magnitude.
The last table 5.13 shows that although the weak AC grid (SCR=1.4), the estimation technique has a reasonably good performance. Estimation error was within 10% except for 600 MW case, where it's about 15.2%.

Transmitted power	error (%) at 150 ms	error (%) at 200 ms
0 MW	25.2	4.7
300 MW	32.2	8.9
600 MW	33.1	15.2
1200 MW	32.9	9.4

Table 5.13: Grid impedance estimation error in (%) in weak grid case SCR=1.4

5.3.6 Comparison between inter-harmonic injection different grid impedance estimation technique

Factor	Inter-harmonic current injection method	RLS algorithm estimation method
Estimation accuracy	The estimation technique performs slightly better for the systems with higher SCC.	The estimation algorithm performs more accurately for grids with smaller SCC compared with the ones with larger SCC.
Estimation time	In both cases of strong and weak grid, the estimation time to reach accuracy (10% or less) was about 200ms.	The execution time of the estimation technique is about 200µS. However, the signals are also to be passed through low pass filter which has a time constant of between 20ms to 50ms. The estimation does not vary much with the filter time constant.
Characteristics of the injected signal	An inter-harmonic signal is need to be injected to the system. However, the disturbance is of minimal effect to the system operation	No disturbance is introduced to the system. The method rely on the generating a regression problem from the measurement of the variations already existed in the system.
Hardware implementation	low computational effort since no complex calculations is required	Low computational efforts. However, it requires two operating points to converge.

Table 5.14: Comparison between inter-harmonic current injection and RLS algorithm methods

6
Conclusion and Future work

6.1 Conclusion

In this thesis the grid impedance estimation techniques have been reviewed. The concept behind each method and the implementation methodology has been examined and explained as well.
Additionally, the advantages and disadvantages of different methods of impedance estimation found in different previous work results were stated. Then, considering not to disturb the stable performance of the power system, a steady-state method based on inter-harmonic current injection was selected for the implementation of the grid impedance estimation. The main goal of this thesis work is to verify the concept of the selected method and it's effectiveness in the estimation of the grid impedance in HVDC applications.
An HVDC model which was developed in PSCAD environment by CIGRE working group B4.57 was used to perform the estimation. The model has been modified by adding the signal generation and impedance calculation algorithm. Also, the grid under test has been designed as a strong grid with SCR = 3 in the first scenario and as a weak grid with SCR = 1.4 in the second case.
Simulations have been performed in different scenarios. These include different frequencies of the injected inter-harmonic signal and different injection axes (the d and q axes). A thorough evaluation of the obtained estimated impedance considering the estimation accuracy and time was presented in the results chapter. In addition to that, cases of impedance estimation with different active and reactive power transmitted have been simulated and the obtained results were presented and discussed.
In the final case, grid impedance estimation of a weak AC system connected to a HVDC system was also conducted. Results have shown that the feasibility of implementing this estimation technique to asses weak ac grids with a reasonable estimation accuracy.

6.2 Future Work

For future work on this topic, I suggest the investigation of possible strategies to improve the estimation accuracy. Also, the speed of the impedance assessing technique is important for HVDC applications because of the bulk power usually transmitted by HVDC system. Therefore, possible improvements on the estimation speed for example, by tuning the
Injection of the inter-harmonic current in both the d and q axes at the same time might also results in different performance of the estimation technique, this aspect might also be in interesting for coming works in the topic.
Another aspect of improvement is to implement an observer to detect any possible changes in grid configuration and trigger the estimation technique and thereby eliminating the manual initiation of the estimation technique.

Bibliography

[1] Mihai Ciobotaru, Remus Teodorescu, Pedro Rodriguez, Adrian Timbus, Frede Blaabjerg. *Online grid impedance estimation for single-phase grid-connected systems using PQ variations.* (2007) Institute of Energy Technology, Aalborg University Pontoppidanstraede 101, 9220 Aalborg.

[2] A.Robert, T.Deflandre. *Guide for Assesing The Network harmonic Impedance.* (1997) Joint CIGRE/CIRED Working Group CC02.

[3] Lucian Asiminoaei, Remus Teodorescu, Frede Blaabjerg,Uffe Borup. *A New Method of On-line Grid Impedance Estimation for PV Inverter.* (2004) Power-Lynx A/S.

[4] MURTY, P. S. R. *power System Analysis* (2017) Butterworth Heinemann

[5] Lucian Asiminoaei, Remus Teodorescu, Frede Blaabjerg, and Uffe Borup *Implementation and Test of an Online Embedded Grid Impedance Estimation Technique for PV Inverters*

[6] Mihai Ciobotaru Remus Teodorescu and Frede Blaabjerg *On-line grid impedance estimation based on harmonic injection for grid-connected PV inverter*(2007)

[7] Pablo García, Mark Sumner, Ángel Navarro-Rodríguez, Juan M. Guerrero, and Jorge Garcia. *Observer-Based Pulsed Signal Injection for Grid Impedance Estimation in Three Phase Systems* Institute of Energy Technology, Aalborg University

[8] Oluwafemi E. Oni, Innocent E. Davidson. *A Review of LCC-HVDC and VSC-HVDC Technologies and Applications* (2016) Electrical, Electronic and Computer Engineering Discipline, University of KwaZulu-Natal Durban, 4001, South Africa, Department of Electric Power Engineering, Durban University of Technology Durban, 4001, South Africa.

[9] Jyoti M. Kharade1, Dr. Niteen G. Savagave2. *A Review of HVDC Converter Topologies*(2017), Department of Electrical Engineering, Annasaheb Dange College of Engineering and Technology Ashta, Maharashtra, India1

[10] A.Gavrilovic' *AC/DC SYSTEM STRENGTH AS INDICATED RY SHORT CIRCUIT RATIOS*

[11] ABB *HVDC Light, It's time to connect: ABB Brochure*

[12] Mohamed H. OkbaJ, Mohamed H. Saiect, M Z. Mostafa3, and T. M Abdel-Moneim3 *High Voltage Direct Current Transmission A Review, Part I* (2012) Egyptian Electricity Transmission Co., Al Behira, EGYPT, Abu-Qir Fertilizers and Chemical Industries Co., Alexandria, EGYPT,Faculty of Engineering, Alexandria University, Alexandria, EGYPT

[13] Ankit Yadav, S N Singh and S P Das *Modular Multi-level Converter Topologies: Present Status and Key Challenges* (2017) Electrical Engineering, Indian Institute of Technology, Kanpur,India

[14] R.S.Geetha, Ravishankar Deekshit, G. Lal *Converter Topologies in VSC-HVDC Systems - an overview*(2014), BMS college of engineering Bangalore, India

[15] Hadi Alyami, Yasser Mohamed *Review and Development of MMC Employed in VSC-HVDC Systems*(2017) Department of Electrical and Computer Engineering, University of Alberta, Edmonton, Canada

[16] Omar Jasim, *Advanced Control Method for VSC-HVDC Systems Connected to Weak Grids* HQS Dang, GE Energy Connection – Grid Solutions, St Leonard's Avenue, Stafford, ST17 4LX, UK

[17] M.C. Di Piazza, P. Zanchetta, M. Sumner, D W P Thomas *Estimation of Load Impedance in a Power System*(2000)

[18] Adrian V. Timbus, Remus Teodorescu,Uffe Borup *Online Grid Impedance Measurement Suitable for Multiple PV Inverters Running in Parallel* Aalborg University, Institute of Energy Technology, PowerLynx A/S, Ellegaardvej 36,, Denmark

[19] Jenny Z. Zhou, Hui Ding, Shengtao Fan, Yi Zhang, and Aniruddha M. Gole. *Impact of Short-Circuit Ratio and Phase-Locked-Loop Parameters on the Small-Signal Behavior of a VSC-HVDC Converter*(2014)

[20] Ali Sheikholeslami *Thévenin and Norton Equivalent Circuits: Part 1*(2018) IEEE SOLID-STATE CIRCUITS MAGAZINE

[21] B.L. THERAJA, A.K. THERAJA *Electrical Technology* (2005) S. CHAND COMPANY LTD.

[22] Cigre Technical brochure 604, *Guide for the Development of Models for HVDC Converters in a HVDC Grid*(2014) WG B4.57, Paris.

[23] Yunhui Huang,Xiaoming Yuan,Jiabing Hu and Pian Zhou. *Modeling of VSC Connected to Weak Grid for Stability Analysis of DC-Link Voltage Control*(2015) IEEE JOURNAL OF EMERGING AND SELECTED TOPICS IN POWER ELECTRONICS, VOL. 3.

[24] S. Meier, *Novel Voltage Source Converter based HVDC Transmission System for Offshore Wind Farms*(2005) Department of Electrical Engineering Electrical Machines and Power Electronics, Royal Institute of Technology, Stockholm.

[25] Lennart Harnefors, Member, IEEE, Massimo Bongiorno, Student Member, IEEE, and Stefan Lundberg, Member, IEEE *Input-Admittance Calculation and Shaping for Controlled Voltage-Source Converters*